

An Optimized Ensemble Deep Learning Model For Brain Tumor Classification

Md. Alamin Talukder^a, Md. Manowarul Islam^a, Md Ashraf Uddin^b

^a*Department of Computer Science and Engineering, Jagannath University, Dhaka, Bangladesh*

^b*School of Information Technology, Deakin University, Waurn Ponds Campus, Geelong, Australia*

Abstract

Brain tumors present a grave risk to human life, demanding precise and timely diagnosis for effective treatment. Inaccurate identification of brain tumors can significantly diminish life expectancy, underscoring the critical need for precise diagnostic methods. Manual identification of brain tumors within vast Magnetic Resonance Imaging (MRI) image datasets is arduous and time-consuming. Thus, the development of a reliable deep learning (DL) model is essential to enhance diagnostic accuracy and ultimately save lives. This study introduces an innovative optimization-based deep ensemble approach employing transfer learning (TL) to efficiently classify brain tumors. Our methodology includes meticulous preprocessing, reconstruction of TL architectures, fine-tuning, and ensemble DL models utilizing weighted optimization techniques such as Genetic Algorithm-based Weight Optimization (GAWO) and Grid Search-based Weight Optimization (GSWO). Experimentation is conducted on the Figshare Contrast-Enhanced MRI (CE-MRI) brain tumor dataset, comprising 3064 images. Our approach achieves notable accuracy scores, with Xception, ResNet50V2, ResNet152V2, InceptionResNetV2, GAWO, and GSWO attaining 99.42%, 98.37%, 98.22%, 98.26%, 99.71%, and 99.76% accuracy, respectively. Notably, GSWO demonstrates superior accuracy, averaging 99.76% accuracy across five folds on the Figshare CE-MRI brain tumor dataset. The comparative analysis highlights the significant performance enhancement of our proposed model over existing counterparts. In conclusion, our optimized deep ensemble model exhibits exceptional accuracy in swiftly classifying brain tumors. Furthermore, it has the potential to assist neurologists and clinicians in making accurate and immediate diagnostic decisions.

Keywords: Deep Learning; Transfer Learning; Optimized; Ensemble; Brain Magnetic Resonance Imaging; Classification

1. Introduction

The brain, a vital organ responsible for all voluntary and involuntary bodily functions, is exceptionally intricate and fragile. Brain tumors, among the most lethal brain disorders, arise from abnormal tissue growth within the skull Engelen et al. (2023); Tseng and Tang (2023). They are classified into primary and secondary tumors, with primary tumors accounting for 70% of cases and remaining confined to the brain Kumar and Kumar (2023); Fares et al. (2023); Cinar et al. (2023). Gliomas, meningiomas, and pituitary tumors are common types, each posing distinct health risks. Pituitary tumors, though typically benign, can cause hormonal imbalances and vision impairment

*Md. Alamin Talukder

Email addresses: alamintalukder.cse.jnu@gmail.com (Md. Alamin Talukder), manowar@cse.jnu.ac.bd (Md. Manowarul Islam), ashraf.uddin@deakin.edu.au (Md Ashraf Uddin)

Salari et al. (2023); Prencipe et al. (2023); Cerbone et al. (2023). Detecting and treating brain tumors present significant challenges due to their complexity and diagnostic intricacies. The World Health Organization forecasts a 5% annual increase in global brain tumor cases Talukder et al. (2023). The blood-brain barrier's protective nature makes conventional radiation detection methods ineffective for detecting tumor growth Hasan et al. (2023). Magnetic resonance imaging (MRI) and computed tomography (CT) scans are preferred clinical tools for identifying brain abnormalities, with MRI being widely utilized across various neurological conditions. Its non-ionizing nature, superior imaging capabilities, and safety profile make MRI the preferred diagnostic modality over CT scans Saeedi et al. (2023); Kimberly et al. (2023); Mukhatov et al. (2023); Duan et al. (2023); Benitez et al. (2024).

In the realm of neuroscience, early detection of brain tumors is crucial, significantly impacting both the preservation of human lives and the efficacy of medical interventions Ale and Nainwal (2023); Luckett et al. (2023). Despite advancements, existing approaches to diagnose irregularities in brain magnetic resonance scans still require enhancement in accuracy and classification speed Alemu et al. (2023). This need is amplified by the escalating volume of medical data, posing challenges to traditional analysis methods Bonate et al. (2023); Chopra et al. (2023). Consequently, the healthcare and medical research community is compelled to optimize methodologies, aiming for more precise clinical insights Li et al. (2023). Deep learning has emerged as a potent tool in this pursuit, leveraging its capacity to autonomously discern complex patterns from vast biomedical datasets, thus revolutionizing disease diagnosis and classification, including brain tumors Marx et al. (2023); Chadha and Verma (2023); Talukder et al. (2024b,a,d)

Deep learning (DL) has revolutionized categorization and prediction, demonstrating exceptional performance in tasks like classification, detection, and voice recognition across diverse domains Talukder et al. (2024c). Its ability to extract intricate patterns from images has significant efficiency and advanced machine learning, especially with large image datasets Nizamani et al. (2023); Rastogi et al. (2024). Unlike traditional methods relying on hand-crafted features, DL automatically optimizes features from raw data, making it appealing for complex biomedical applications and positioning it as a leading technique for image-based tasks Talukder et al. (2022); Zheng et al. (2023). Transfer learning (TL) is instrumental in reducing computational resources by leveraging pre-existing model knowledge, enabling expedited model training and optimization through the adaptation of pre-trained model weights, particularly in convolutional layers Talukder et al. (2023); Andreas et al. (2023). TL can serve various purposes, such as serving as a foundational model for object classification, extracting features, or fine-tuning for specific data sources, facilitating the development of specialized models for diverse applications Dewi et al. (2023); Kumar et al. (2023); Zulfiqar et al. (2023).

In the extensive body of related works, each effort stands as a unique approach to the category of brainiac tumors, contributing valuable insights to the field Ayadi et al. (2021). Moreover, DL techniques have found notable applications in representing and interpreting various medical images Sadad et al. (2021). These methods have empowered machines to effectively assess a wide array of medical data, ranging from multidisciplinary pathology scans to elevated-dimensional image datasets and video recordings, as exemplified in the work of Qureshi et al. (2023); Sharma et al. (2023). Furthermore, the versatility of DL extends its impact beyond medical imaging to encompass disease prediction. Researchers such as Singh and Agarwal (2023); Kumari et al. (2023); Al-Azzwi and Nazarov (2023) have demonstrated the adaptability of DL techniques in healthcare, offering fresh insights into the

intersection of DL and disease prediction. These collective contributions underscore the wide-ranging applications of DL in medical research, providing a strong foundation for our innovative approach to categorizing brain tumors Al-Zoghby et al. (2023); Muezzinoglu et al. (2023); Emam et al. (2023).

The manual assessment and analysis of an extensive collection of brain MRI data is resource-intensive, time-consuming, and prone to errors, given the expertise required for processing and classifying MRI images. The precise diagnosis and categorization of brain tumors are crucial as they inform prognostic predictions and guide medical experts in selecting suitable treatment options. However, the manual evaluation of diverse brain MRI data is prone to inaccuracies and demands considerable expertise. This precision in diagnosis and categorization is imperative as it underpins predictive insights and empowers medical specialists to make well-informed decisions regarding patient care.

Our research aims to construct a robust Deep Learning (DL) model for efficient brain tumor prediction from MRI data. We establish a systematic framework involving preprocessing, Transfer Learning (TL) fine-tuning, layer addition, and DL model ensemble. We optimize this ensemble using Genetic Algorithm-based Weight Optimization (GAWO) and Grid Search-based Weight Optimization (GSWO). The Pivotal TL architectures like ResNet50V2, ResNet152V2, Xception, and InceptionResNetV2 are selected for their computational efficiency and proven efficacy in handling MRI complexities, crucial for processing large brain tumor datasets.

The main contributions of this research are:

1. We introduce an optimized DL model specifically designed for categorizing brain tumors. This model incorporates comprehensive preprocessing steps, TL architecture modifications, fine-tuning techniques, and optimization-based ensemble techniques, significantly enhancing classification efficiency.
2. We refine the TL architecture by integrating advanced image augmentation techniques to address overfitting concerns and capitalize on GPU acceleration. Additionally, we introduce image standardization to streamline the augmentation process, enhancing workflow efficiency.
3. We employ an ensemble approach with weight optimization techniques, including grid search and genetic algorithms on the fine-tuned DL models for efficient brain tumor classification to develop highly accurate predictive models.

The following sections of the paper are organized as follows: Section 2 provides an overview of previous studies on the predicting of brain tumors using deep learning. Section 3 explains our research methodology and dataset in detail. In Section 4, we present the experimental setup and performance evaluation. Finally, the paper concludes with Section 5.

2. Literature Review

The category of brain tumors is pivotal for accurate assessment and the formulation of targeted treatment strategies based on their specific types. Neuroimaging techniques, notably MRI, are widely employed to identify brain cancers precisely. The preference for MRI stems from its unparalleled image quality and the absence of ionizing radiation. Within ML, DL is a subset renowned for its proficiency in classification and detection tasks—consistently yielding noteworthy outcomes.

Talukder et al. (2023) introduced a new DL approach for categorizing brain tumors. The method involved various steps such as data preprocessing, TL architecture creation, and fine-tuning. They tested different TL models like Xception, ResNet50V2, InceptionResNetV2, and DenseNet201 on Figshare data with 3,064 MRI brain tumor images. The results demonstrated high accuracy, with ResNet50V2 achieving the best performance at 99.68%. This outperformed other models and could help doctors diagnose brain tumor patients quickly and accurately.

Asif et al. (2023) designed a brain tumor diagnosis system using DL architectures, including DenseNet121, ResNet152V2, Xception, DenseNet201 and InceptionResNetV2. Modifications to the final layers, incorporating a deep dense block and softmax layer, aimed to enhance classification accuracy. Two experiments were conducted: one involving three-class classification (glioma, meningioma, and pituitary tumors) and another with four classes (including healthy patients). The outcomes emphasize the authority of the presented model based on the Xception architecture, achieving a remarkable 99.67% accuracy in the three-class dataset and 95.87% in the four-class dataset, outperforming state-of-the-art methods. This model holds promise as an automated diagnostic tool for radiologists, enabling and accurate decision-making.

Nassar et al. (2023) prepared an efficient automated approach to assist radiologists in classifying brain tumors, intending to save time compared to manual image analysis. The approach utilized 3064 brain MRI images from 233 patients. Drawing on the results of five different models, such as GoogleNet, ShufNet, SqueezeNet, AlexNet and NASNet-Mobile, the system harnessed the integrated possibility of numerous models and performed a majority voting technique to acquire favorable outcomes. The offered method demonstrated substantial progress in results, achieving an impressive prevalent exactness of 99.31%.

In the research conducted by Tummala et al. (2022), ImageNet-based Vision Transformer (ViT) models were employed, having undergone pre-training and fine-tuning for categorization tasks. The ensemble ViT model's interpretation was assessed using the Figshare brain tumor dataset, specifically for a three-class classification task through cross-validation (CV) and testing. The amalgamation of all ViT variants such as L/16, B/16, L/32, and B/32—achieved an impressive total testing accuracy of 98.7%. This suggests that a group of ViT models holds the potential to aid in the marker of brain cancers based on MRI images, offering support to radiologists.

Abd El-Wahab et al. (2023) developed BTC-fCNN, a DL-based system for efficiently classifying three types of brain tumors—meningioma, glioma, and pituitary tumors—using MRI images from the Figshare dataset. The model, with 13 layers incorporating convolution and 1×1 convolution layers, average pooling, fully connected layers, and a softmax layer, underwent five iterations, incorporating TL and five-fold cross-validation. The presented model attained remarkable results, boasting an average accuracy of 98.63% with five iterations and TL and 98.86% with retrained five-fold cross-validation. BTC-fCNN outperformed existing strategies and other well-known CNNs, significantly advancing in categorizing brain tumors.

Maruf et al. (2022) conducted a thorough assessment of 26 previously developed CNN models designed for general image classification in the context of the brain tumor category. The evaluation involved retraining these models using 3064 T1-weighted contrast-enhanced MR images. Pre-trained weights from the ImageNet dataset were employed, and the classification accuracies of the CNN models were compared. This comprehensive study examines various state-of-the-art CNN models using a multiclass brain MRI dataset. EfficientNetB3 emerged as the top performer, achieving a categorization accuracy of 98.98% among the 26 models tested. Other models,

including DenseNet121, EfficientNetB2, EfficientNetB5, and EfficientNetB4, also demonstrated strong accuracy, with all models surpassing 97% accuracy in identifying the tumor type. This research delivers helpful discernment into the efficacy of diverse CNN models for categorizing brain tumors.

Saeedi et al. (2023) developed a 2D CNN and a convolutional auto-encoder network, both trained with designated hyperparameters. The 2D CNN comprised multiple convolution layers, all utilizing a 2*2 kernel function. This hierarchical network included eight convolutional and four pooling layers, with batch-normalization layers applied after all convolution layers. The revised auto-encoder network incorporated a convolutional auto-encoder and a classification convolutional network utilizing the last output encoder layer from the first part. Additionally, six ML techniques for categorizing brain tumors were analogized in this study. Results revealed a training accuracy of 96.47% for the presented 2D CNN and 95.63% for the offered auto-encoder network. The average recall values were 95% for the 2D CNN and 94% for the auto-encoder network. The study concluded that the proposed 2D CNN accurately classified brain tumors.

To optimize hyperparameters for CNN, Ait Amou et al. (2022) presented an advanced strategy relying on Bayesian optimization. Tested in the categorization of brain MRI scans into three cancer classes, the CNN, optimized using five pre-trained instances through TL, achieved a remarkable accuracy rate of 98.70% after employing Bayesian optimization. The proposed model surpassed existing works, showcasing the effectiveness of automated hyperparameter optimization.

Ayadi et al. (2021) showcased a CNN-based model with multiple layers for MRI categorizing brain tumors. Requiring minimal preprocessing, the intelligent model was evaluated on three distinct brain tumor datasets. Achieving accuracy rates of 94.74 percent for Figshare, 93.71 percent for Radiopaedia, and 97.22 percent for Rembrandt datasets, the proposed scheme demonstrated superior classification and recognition accuracies compared to previous relevant studies on the same data.

Ayadi et al. (2021) introduced an advanced CNN model with multiple layers designed specifically for MRI-based categorizing brain tumors. This innovative model required only minimal preprocessing and was rigorously tested across three different brain tumor datasets. The results were remarkable, with the model attaining accuracy rates of 94.74% on the Figshare dataset, 93.71% on the Radiopaedia dataset, and 97.22% on the Rembrandt dataset. These performance metrics underscored the model's capability in classifying and recognizing brain tumors, significantly improving over previous studies conducted using the same datasets.

3. Methodology

In this study, we propose an optimized Deep Learning (DL) approach for the accurate classification of brain tumors using a publicly accessible dataset from Figshare MRI. Our methodology represents a significant advancement in the field by introducing a comprehensive framework that integrates various stages of preprocessing, Transfer Learning (TL) architecture modification, fine-tuning, and ensemble DL models. This holistic approach aims to significantly enhance the efficiency and accuracy of brain tumor classification. Unlike existing methods, our model incorporates architectural refinements such as image augmentation techniques to mitigate overfitting and improve generalization performance. Additionally, we implement image standardization to streamline the preprocessing

workflow and capitalize on the computational advantages of Graphics Processing Units (GPUs). Through meticulous fine-tuning, we tailor the TL architectures to better capture subtle features indicative of brain tumors, thereby enhancing classification accuracy. Furthermore, we introduce an ensemble approach coupled with weight optimization techniques, including grid search and genetic algorithms, to further enhance the predictive power of our model. In this section, we delineate our presented methodology, outlining the application of various TL algorithms within our framework. Initially, we elucidate the operational principles of our proposal, followed by a concise overview of the TL algorithms employed.

To facilitate the prognosis of brain tumors, our approach encompasses image data collection, preprocessing, and a TL architecture with reconstruction. The architecture is fine-tuned by adding supplementary layers such as batch normalization, global average pooling, dense+ReLU, flatten, drop out, and dense+Softmax layers for categorizing brain tumors on a dedicated dataset. Fig 1 and Fig 2 illustrate our proposed paradigm’s schematic representation and structural design, respectively. The procedural steps of our presented approach are enumerated as follows:

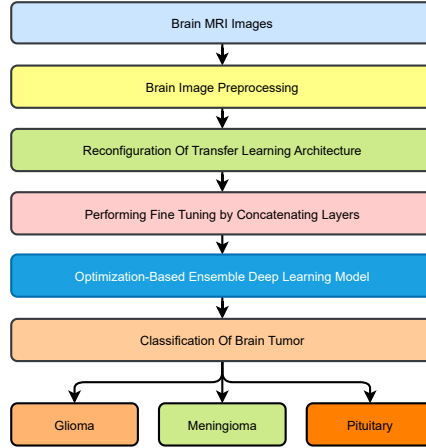


Figure 1: The schematic representation of our proposed research approach

- **Step-1:** Commencing the experiment, we initiate with the brain tumor dataset, comprising three distinct types of tumors: meningioma, glioma and pituitary.
- **Step-2:** In the pre-processing phase, the images undergo resizing to achieve a standardized dimension of 256x256. Subsequently, a sharpening filter is applied, followed by image complementation and scaling to standardize the picture data.
- **Step-3:** In the reconstruction transfer learning architecture, image augmentation is introduced after the input layer, and the model is refined by truncating the last layers post the activation layer.
- **Step-4:** Further refinement is achieved through fine-tuning, involving the attachment of additional layers such as global average pooling, batch normalization, flattening, dropout, and dense layers with ReLU and SoftMax activations, enhancing the model’s suitability for categorizing brain tumors.
- **Step-5:** The integration of well-established TL algorithms, including ResNet50V2, ResNet152V2, Xception, and InceptionResNetV2, is implemented to bolster the performance of our approach.

- **Step-6:** Employing an ensemble approach, we combine predicted models and optimize the ensemble through two techniques: genetic optimization and grid search-based weighted optimization.
- **Step-7:** The evaluation stage involves assessing the interpretation of each fine-tuned TL model and the two optimized ensemble models. Metrics such as Recall, Precision, F1-score, Accuracy, Confusion Matrix, MCC, Kappa, and CSI are utilized. The selection of the best model is based on comprehensive performance analysis. Additionally, a comparative assessment is conducted with existing works.

3.1. Data collection

The brain tumor dataset, sourced from Cheng (2017), encompasses 3064 T1-weighted contrast-enhanced images derived from 233 patients afflicted with three distinct types of brain tumors: meningioma (708 slices), glioma (1426 slices), and pituitary tumor (930 slices). This comprehensive dataset is conveniently available in Matlab file format (.mat file). Each file is structured as a Matlab struct, encapsulating crucial information for each image, including labels 1, 2 and 3 for meningioma, glioma, and pituitary tumors respectively, Image data, patient ID (PID) and tumor border. The tumor boundary, meticulously traced manually and represented as a vector of coordinates along the tumor’s edge, facilitates the straightforward production of a binary image for the tumor mask. The data includes a tumor mask, presented as a binary image wherein a string of ones identifies the tumor region.

This dataset is beneficial for research and experimentation in brain tumor categorization. Figure 3 visually illustrates the distribution of this dataset, providing insights into the composition of the three tumor types across the patient cohort.

3.2. Image pre-processing

We meticulously prepared the dataset for further analysis in the initial stages of image preprocessing. Since the data was initially stored in Matlab (.mat) file format, we extracted image and label information to facilitate subsequent processing. The image preprocessing journey commenced with resizing all images to a uniform 256x256 dimension, enhancing visibility by applying a sharp filter and complementing the images. Further refinement was achieved through histogram equalization, contributing to a more balanced image representation. To ensure compatibility with the Convolutional Neural Network (CNN) model, we scaled the images by dividing them by 255. For effective model training and evaluation, we performed k-fold cross-validation where k is five, so the dataset is partitioned into training, testing, and validation sets, allocating 80%, 10%, and 10%, respectively. Additionally, we applied 1000 shuffling iterations to reduce loss, lower variance, and enhance the model’s generalization. The resultant processed images exhibit heightened sharpness, brightness, and discernible details compared to their original counterparts, making them well-suited for input into the model. This meticulous preprocessing contributes to achieving an outstanding performance compared to contemporary methodologies.

Figure 4 visually elucidates the sequential steps of image preprocessing for distinct brain tumor types such as meningioma, glioma and pituitary. The upper section of the figure (a, b, c) showcases images before preprocessing, while the lowest section (d, e, f) portrays the same images after the application of preprocessing steps.

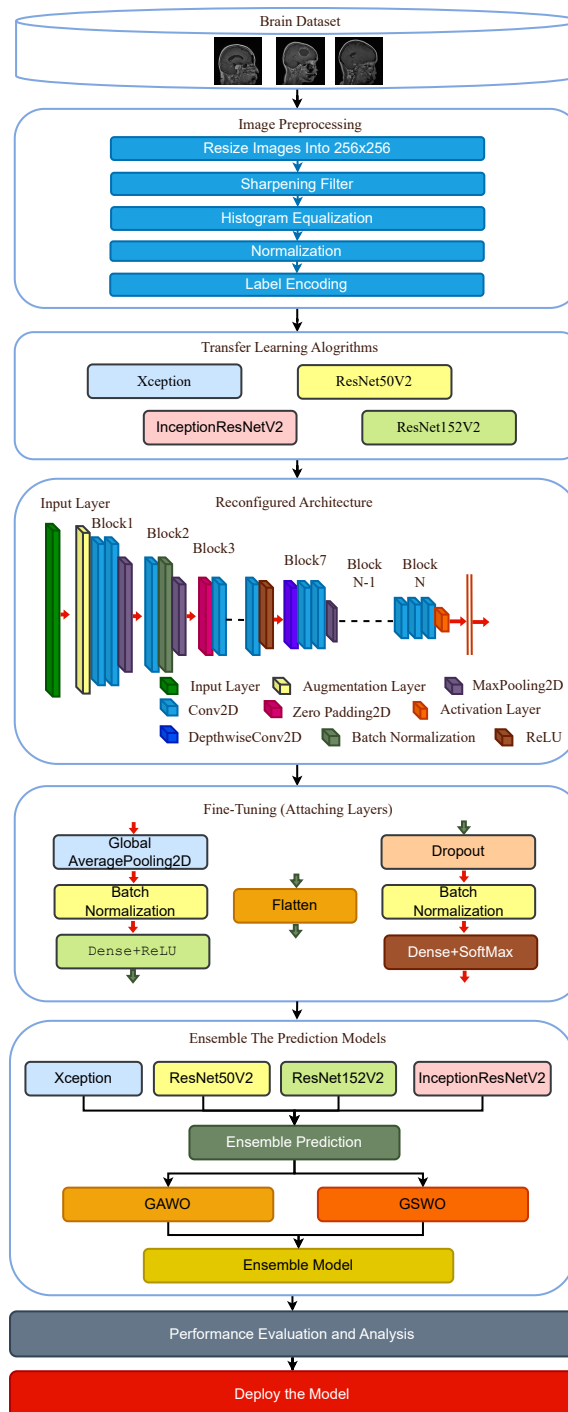


Figure 2: The proposed structural design for classifying brain tumors

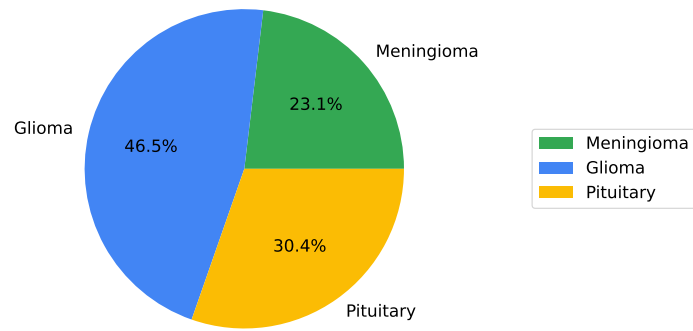


Figure 3: The distribution pattern of brain tumor data collection

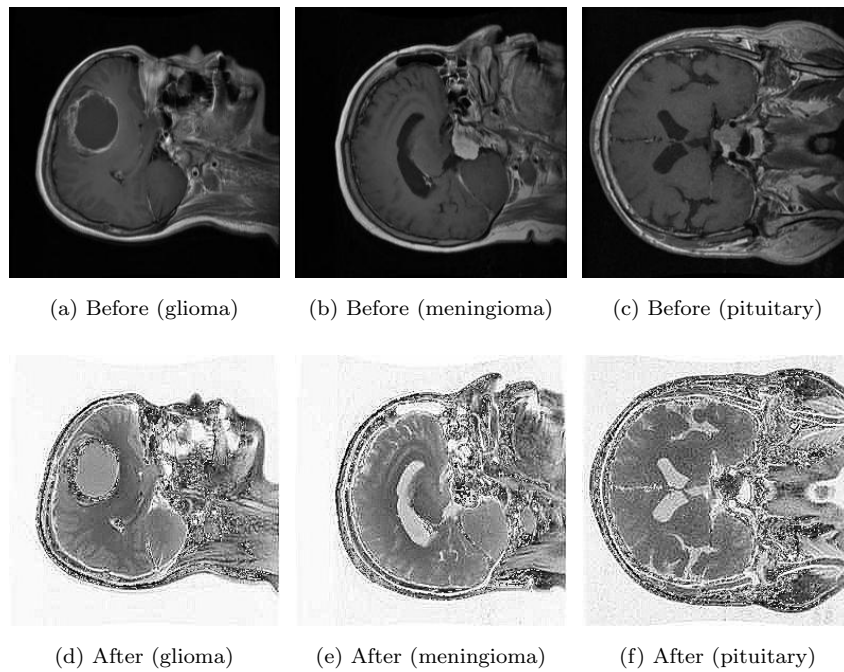


Figure 4: Images of brain glioma, meningioma, and pituitary tumors prior to and following image preprocessing

3.3. Reconstruction with Fine-Tuning of transfer learning architecture

In our experimental endeavor, we undertake the crucial tasks of reconstructing TL models and fine-tuning them to enhance the model’s aptitude for accurately categorizing brain tumors. Within the reconstruction TL architecture framework, we address the inherent challenge posed by pre-trained TL algorithms, originally trained on ImageNet data You et al. (2020). To adapt these algorithms for our specific brain tumor dataset, we embark on a reconstruction process to optimize the architecture for better predictions. This reconstruction unfolds in two sequential steps:

- **Image Augmentation:** Initially, we incorporate an image augmentation layer into the input layer of our architecture. This integration allows the architecture to perform on-device image augmentation concurrently with other layers, taking advantage of GPU acceleration for expedited processing. Moreover, by preserving pre-processing layers alongside the model, we ensure instantaneous standardization of images during deployment, eliminating the need for redundant server-side logic.
- **Truncate Layers:** Subsequently, we retain all layers from the TL algorithms, excluding those beyond the last activation layer. This strategic truncation is performed to accommodate the addition of extra layers, optimizing the architecture for efficient brain tumor prediction.

Figure 5 visually illustrates the juxtaposition of the original and reconfigured TL architectures. Figure 5(a) delineates the original TL architecture. In contrast, Figure 5(b) showcases the reconfigured architecture and fine-tuning process, showcasing the iterative refinement process undertaken to tailor the model for precise categorizing brain tumors.

3.3.1. Image Augmentation

The image augmentation process is seamlessly integrated into our proposed architecture. Recognizing the pivotal role of image augmentation in enriching dataset scale and diversity, we leverage this technique to amplify the effectiveness of our DL models. In our approach, we implement image processing techniques on the input images, generating augmented counterparts. The augmentation process encompasses fundamental transformations such as zooming, rotation, contrast adjustment and horizontal flipping. Additionally, the input images undergo rescaling to a standardized range of 0 to 1, fostering optimal conditions for model training.

This deliberate incorporation We introduced additional random rotations and translations to enhance the variety of our augmented data dataset and bolster the model’s adaptability to varying real-world scenarios. Figure 6 serves as a visual testament to the augmentation process, highlighting its integral role in refining the efficacy of our proposed deep learning architecture.

To enhance the variety of our augmented data, we introduced additional random rotations and translations. The image augmentation process, embedded within the TL architecture, unfolds through the following meticulously adjusted techniques:

- **Horizontal Flip Function:** This function flips the image horizontally at random, applicable to images with a 256x256x3 dimension, where ‘256’ refers to both height and width and ‘3’ signifies the RGB colour channels.

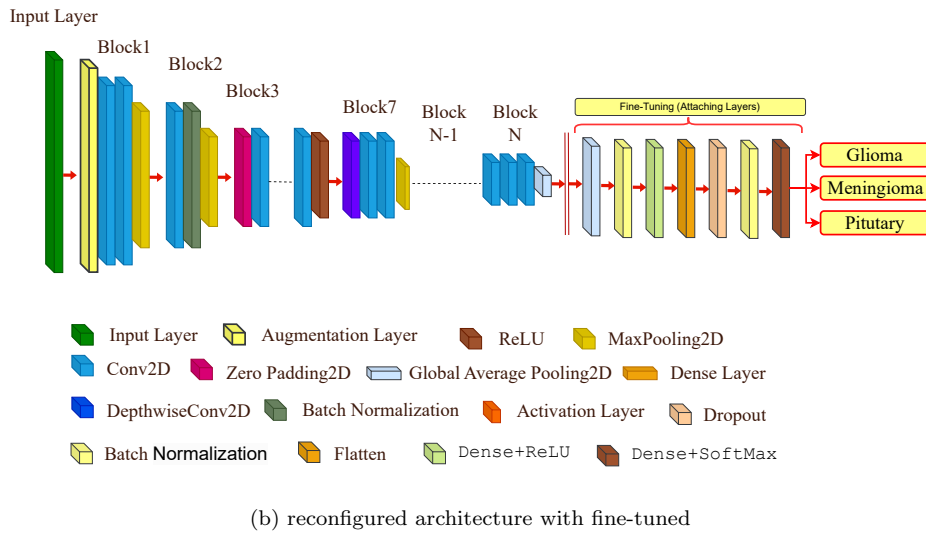
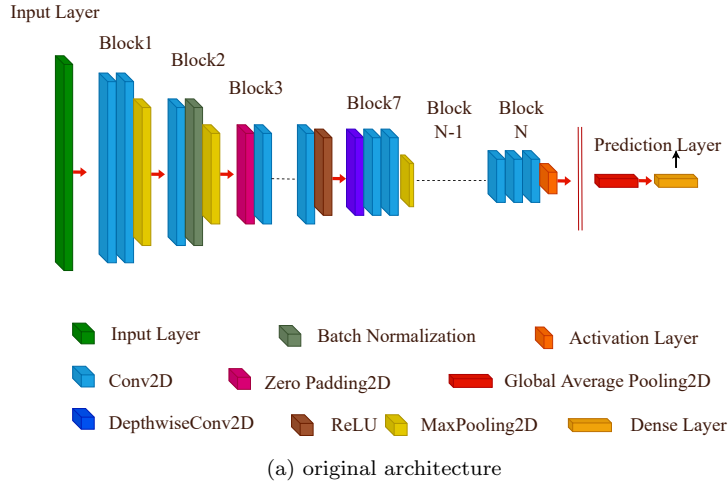


Figure 5: The original and reconfigured with fine-tuned architecture of transfer learning model

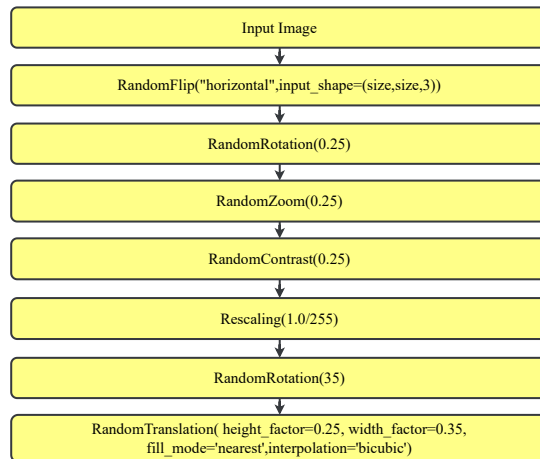


Figure 6: The augmentation process of our proposed architecture

- **Random Image Rotation:** Allows the image to rotate randomly, with a limit of 0.25 radians.
- **Image Zoom Adjustment:** Enables random zooming in or out on the image, up to a maximum of 25%.
- **Contrast Variation:** Alters the contrast of the image randomly, up to a maximum change of 25%.
- **Pixel Rescaling:** Adjusts the image’s pixel values, rescaling them to a range between 0 and 1.
- **Degree-Based Image Rotation:** This function randomly rotates the image, with a maximum rotation of 35 degrees.
- **Image Translation with Parameters:** Randomly shifts the image horizontally and vertically by up to 25% and 35% of the image’s height and width, respectively. The translation uses the ‘nearest’ fill mode to handle pixels outside the boundary and ‘bicubic’ interpolation for the better visual quality of the transformed image.

This meticulously refined augmentation process ensures that the augmented dataset maintains heightened diversity while remaining a faithful representation of original MRI images. The outcome-augmented dataset is the cornerstone for training our presented model, attaining state-of-the-art performance in the targeted task. Consequently, these advanced image-processing strategies augment data proportions and significantly enhance assortment, thereby elevating the overall rendition of DL algorithms.

3.3.2. Fine-Tuning Process

In the fine-tuning phase, we enhance the architecture by introducing specific layers tailored to the characteristics of brain MRI images. Our refined structural design includes a Global Average Pooling2D layer, two Batch Normalization layers, a Dense layer with ReLU and SoftMax activation, a flattened layer, and a Dropout layer to optimize model performance. The Global Average Pooling2D calculates the average output for each feature map across the entire spatial dimensions, reducing spatial dimensions to 1x1, capturing global context, reducing parameter count, and ensuring translation invariance. Batch Normalization standardizes layer inputs, reducing internal covariate shift, enhancing training stability, accelerating convergence, mitigating gradient issues, and providing regularization. The Dense layer followed by ReLU activation introduces non-linearity, enhancing model expressiveness, enabling learning of complex relationships, and capturing intricate patterns. The flattened layer converts the multi-dimensional output into a one-dimensional array, facilitating input compatibility with subsequent layers and ensuring information flow continuity. Dropout randomly deactivates neurons to prevent overfitting, improve generalization, enhance robustness, and reduce overfitting risks. Another instance of Batch Normalization provides additional normalization and regularization, further stabilizing training, enhancing generalization, and contributing to model robustness. The final Dense layer with SoftMax activation produces probability distributions over classes, facilitating accurate classification, and is well-suited for multi-class tasks. Pre-trained trainable weights are incorporated to leverage existing knowledge, and the model is configured with the Adamax optimizer, setting a learning rate of 0.0001 for efficiency in handling embeddings and stability enhancement. The loss function is set to sparse categorical cross-entropy, suitable for integer-form labels obtained through label encoding, with accuracy as the primary performance metric. This comprehensive fine-tuned architecture, with a Flatten and Dropout layer, effectively captures brain MRI data intricacies while addressing overfitting concerns.

3.4. Transfer Learning Algorithms

In our experimentation, we employed four TL algorithms for categorizing brain tumors. Utilizing the knowledge gained from these TL models, we integrated two optimization approaches to tailor the proposed models to our objectives.

- Xception Architecture:

The Xception framework, often called "Extreme Inception," is a unique convolutional neural network structure, as described in Chollet (2017). It is distinguished by its depthwise separable convolution layers arranged in a series and the integration of residual connections. The design comprises 36 convolution layers that are grouped into 14 distinct modules. Each module, except for the first and last, is connected through linear residual links. The simplicity of Xception, which is easily implemented using frameworks such as Keras Joseph et al. (2021) or TensorFlow-Slim Tian et al. (2020), contrasts the complexity of architectures like InceptionV2 or V3.

- ResNet50V2:

The ResNet model, a pioneering neural network introduced by He et al. (2016a), has shown remarkable success, notably in the ILSVRC 2015 classification challenge. ResNet50, a variant with 50 layers, uses deep residual networks with "skip connections" for accuracy. The ResNet50V2, an evolution of the original ResNet50, demonstrates better performance on the ImageNet dataset, as noted in He et al. (2016b) and Rahimzadeh and Attar (2020). It introduces an optimized connection structure between blocks, boosting overall performance.

- ResNet152V2:

Building upon the ResNet50 model, ResNet152V2 extends the depth to 152 layers, capturing more complex data features, as detailed in Bhosale and Patnaik (2023). It maintains the original ResNet's use of residual blocks and skip connections, proven effective in vision tasks. The model's design, including skip connections in residual blocks, contributes to its robustness, facilitating the efficient training of deep architectures, as discussed in Rakshit et al. (2023).

- InceptionResNetV2:

The InceptionResNetV2 design, an advancement over InceptionResNetV1, combines residual learning with the inception block structure, as outlined in Szegedy et al. (2017). It includes various block types like the Stem, InceptionResNet, and Reduction blocks. The network's depth, achieved through an intricate arrangement of these blocks, ensures high-quality feature extraction and processing, further elaborated in Asif et al. (2022).

The selection and modification of transfer learning (TL) architectures, including ResNet50V2, ResNet152V2, Xception, and InceptionResNetV2, for brain tumor classification, were grounded in the pursuit of maximizing classification accuracy while mitigating computational complexity. Each TL architecture was chosen for its proven efficacy in image classification tasks and its ability to capture intricate features within the data. To adapt these architectures to the characteristics of the brain tumor dataset, specific methodologies were employed. Firstly, the pre-trained weights of the TL architectures were fine-tuned using the brain tumor dataset to ensure that the models could effectively discern relevant features from MRI images. Additionally, architectural refinements such as the incorporation of image augmentation techniques and the addition of tailored layers were implemented to enhance

the models' capacity to detect subtle patterns indicative of brain tumors. These modifications were validated through rigorous experimentation, including cross-validation techniques and evaluation metrics such as precision, recall, F1-score, and accuracy, ensuring that the reconstructed TL architectures effectively captured the nuances of the brain tumor dataset while maintaining robust performance across diverse evaluation criteria.

3.5. Adopted Optimization Methods

In our experiment, along with four reconstructed and fine-tuned TL models, we incorporate two ensemble approaches such as Genetic algorithm-based weighted optimization (GAWO) and Grid search-based weighted optimization (GSWO), to make the prediction more accurate in classifying brain tumors.

The rationale behind selecting genetic algorithm-based weighted optimization (GAWO) and grid search-based weighted optimization (GSWO) methods for ensemble model optimization, it's crucial to underscore the strategic considerations driving this choice. The adoption of GAWO and GSWO stems from their distinct advantages in handling optimization tasks within ensemble learning frameworks. GAWO, harnessing principles inspired by natural selection, offers a powerful mechanism for exploring complex solution spaces and adapting model weights iteratively. On the other hand, GSWO operates through an exhaustive search strategy, systematically evaluating model configurations to identify the most effective ensemble combinations.

The decision to employ these methodologies was driven by their complementary strengths. GAWO's ability to efficiently navigate high-dimensional parameter spaces aligns well with the intricate optimization requirements of ensemble models. Conversely, GSWO's systematic exploration ensures thorough coverage of potential configurations, enhancing the likelihood of identifying optimal solutions. In determining the parameters and convergence criteria for these optimization methods, meticulous experimentation and validation were conducted. Parameters such as population size, mutation rates, and convergence thresholds were fine-tuned through iterative testing to strike a balance between exploration and exploitation within GAWO. Similarly, for GSWO, parameters governing grid granularity and search bounds were optimized to facilitate comprehensive exploration while mitigating computational overhead. Considerations for computational efficiency and model stability played a pivotal role throughout the optimization process. Efforts were directed towards optimizing algorithmic parameters to ensure efficient resource utilization, minimizing computational burden without compromising optimization efficacy. Additionally, convergence criteria were carefully defined to prevent premature convergence or instability, thereby fostering robust model performance. By adopting GAWO and GSWO within our ensemble model optimization framework, we aimed to leverage their respective strengths to enhance the accuracy and robustness of our classification system, ultimately contributing to better diagnostic outcomes in the realm of brain tumor classification.

The fitness function utilized in the genetic algorithm (GA) plays a pivotal role in evaluating potential solutions to the weight optimization problem. Specifically, the fitness function assesses the quality of candidate solutions by quantifying their performance in terms of accuracy on a designated test dataset. For our brain tumor classification task, the fitness function calculates the accuracy of ensemble predictions generated by combining the outputs of individual models weighted according to the candidate solution. The objective is to maximize accuracy, thereby identifying the most effective combination of model weights for achieving superior classification performance. Importantly, the fitness function is designed to assign higher fitness scores to solutions that yield higher ensemble

accuracy, incentivizing the GA to converge towards optimal solutions over successive generations.

While GAs were initially chosen for weight optimization due to their efficiency in exploring complex solution spaces, further experimentation revealed that grid search-based optimization outperformed GAs in terms of both performance and computational time. Grid search systematically evaluates a predefined grid of weight combinations, offering simplicity and transparency in exploring the solution space. This approach proved to be highly effective in identifying optimal ensemble configurations while requiring less computational time compared to GAs. Additionally, grid search exhibited robust performance across different optimization tasks and settings, making it a favorable choice for weight optimization in our ensemble learning framework. Thus, despite the initial consideration of GAs, the superior performance and computational efficiency of grid search ultimately led to its adoption as the preferred optimization technique for weight optimization in our study.

4. Results and Discussion

Our methodology involves refining the TL architecture by fine-tuning and adding extra layers to boost its efficiency, where we utilized four distinct TL algorithms and developed two ensemble DL models based on optimization techniques. These models were specifically designed to evaluate our approach’s capability in detecting brain tumors. To estimate our strategy’s performance, we used various performance metrics. The following section will provide an in-depth look at the experimental framework, the criteria used for evaluating performance, an analysis of the outcomes, and an extensive review of the results we obtained.

4.1. Experiment Setup

This research was carried out using a computer equipped with an Intel Xeon CPU, including three cores, 30GB of RAM, a GPU with 30GB memory, and a 70GB hard disk. For the experimental setup, a Jupyter notebook was utilized. The proposed method was implemented in Python, using well-known libraries such as Scikit-learn, scikit-image, Keras, TensorFlow, Seaborn, Matplotlib, Numpy, and Pandas.

4.2. Metrics for Evaluating Model Performance

Our methodology’s effectiveness is rigorously evaluated using a range of metrics. These include accuracy, precision, recall, F1-score, the confusion matrix, Matthews correlation coefficient (MCC), Kappa, and the Classification Success Index (CSI). Each of these metrics provides a distinct perspective on the model’s ability to classify data accurately.

- **Confusion Matrix:** This matrix format presents the values of True Positives (TP), True Negatives (TN), False Positives (FP), and False Negatives (FN). It serves as a foundation for assessing accuracy, precision, recall, and the F1-score (refer to Table 1).
- **Accuracy:** This statistical measure evaluates the proportion of correctly identified instances in relation to the overall dataset.

$$Accuracy = \frac{TP + TN}{TP + FP + FN + TN} \tag{1}$$

	Actual Positive	Actual Negative
Predicted Positive	TP	FP
Predicted Negative	FN	TN

Table 1: Confusion Matrix

- **Precision:** This metric calculates the fraction of correctly predicted positive observations out of all the positive predictions made.

$$Precision = \frac{TP}{TP + FP} \quad (2)$$

- **Recall:** Recall, also known as sensitivity, determines the fraction of actual positives that are correctly identified.

$$Recall = \frac{TP}{TP + FN} \quad (3)$$

- **F1-Score:** The F1-score is the harmonic mean of precision and recall, providing a balance between these two metrics.

$$F1_{score} = 2 * \frac{(Recall * Precision)}{(Recall + Precision)} \quad (4)$$

- **Matthews Correlation Coefficient (MCC):** MCC is a reliable statistical rate that evaluates the quality of binary classifications. It ranges from -1 (total disagreement) to 1 (perfect agreement).

$$MCC = \frac{(TPTN) - (FPFN)}{\sqrt{(TP + FP)(TP + FN)(TN + FP) * (TN + FN)}} \quad (5)$$

- **Kappa:** Kappa coefficient indicates the level of consistency between predicted and actual classifications, accounting for random chance.

$$Kappa = \frac{(P_o - P_e)}{(1 - P_e)} \quad (6)$$

Here, P_o is the observed agreement, and P_e is the expected agreement by chance.

$$P_o = \frac{(TP + TN)}{(TP + TN + FP + FN)} \quad (7)$$

$$P_e = \frac{((TP + FP) * (TP + FN) + (TN + FP) * (TN + FN))}{(TP + TN + FP + FN)^2} \quad (8)$$

- **Classification Success Index (CSI):** CSI calculates the ratio of accurately classified instances against the total number of classifications.

$$CSI = \frac{TP}{TP + FP + FN} \quad (9)$$

4.3. Evaluation of Results and Analysis of Model Performance

In our study, we applied four advanced TL algorithms and two optimized ensemble DL models, aiming for precise classification of brain tumors within our dataset. The results of this application are presented in Table 2 and illustrated in Figure 7, which details the performance metrics and error rates of our refined and ensemble models. As shown in 7(a), the accuracy figures for Xception, ResNet50V2, ResNet152V2, InceptionResNetV2,

GAWO, and GSWO are 99.42%, 98.37%, 98.22%, 98.26%, 99.71%, and 99.76% respectively. Similarly, the precision statistics are 99.43%, 98.41%, 98.34%, 98.37%, 99.71%, and 99.77%; recall figures are 99.42%, 98.37%, 98.22%, 98.26%, 99.71%, and 99.76%; and the f1-score rates are 99.43%, 98.41%, 98.34%, 98.37%, 99.71%, and 99.77% for the same models, respectively. Notably, the GSWO model exhibited the highest performance levels, achieving an accuracy of 99.76%, precision of 99.77%, recall of 99.76%, and an f1-score of 99.77%.

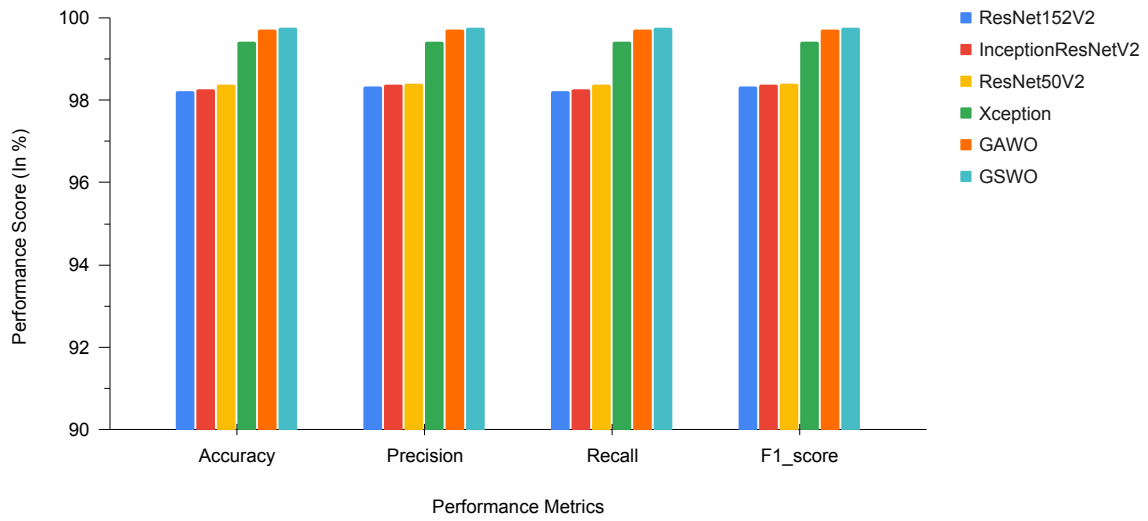
SN.	Model Name	Accuracy	Precision	Recall	F1_score	MCC	Kappa	CSI
0	Xception	99.42	99.43	99.42	99.43	99.42	99.43	99.42
1	ResNet50V2	98.37	98.41	98.37	98.41	98.37	98.41	98.37
2	ResNet152V2	98.22	98.34	98.22	98.34	98.22	98.34	98.22
3	InceptionResNetV2	98.26	98.37	98.26	98.37	98.26	98.37	98.26
4	GAWO	99.71	99.71	99.71	99.71	99.71	99.71	99.71
5	GSWO	99.76	99.77	99.76	99.77	99.76	99.77	99.76

Table 2: Performance Analysis of Proposed Models

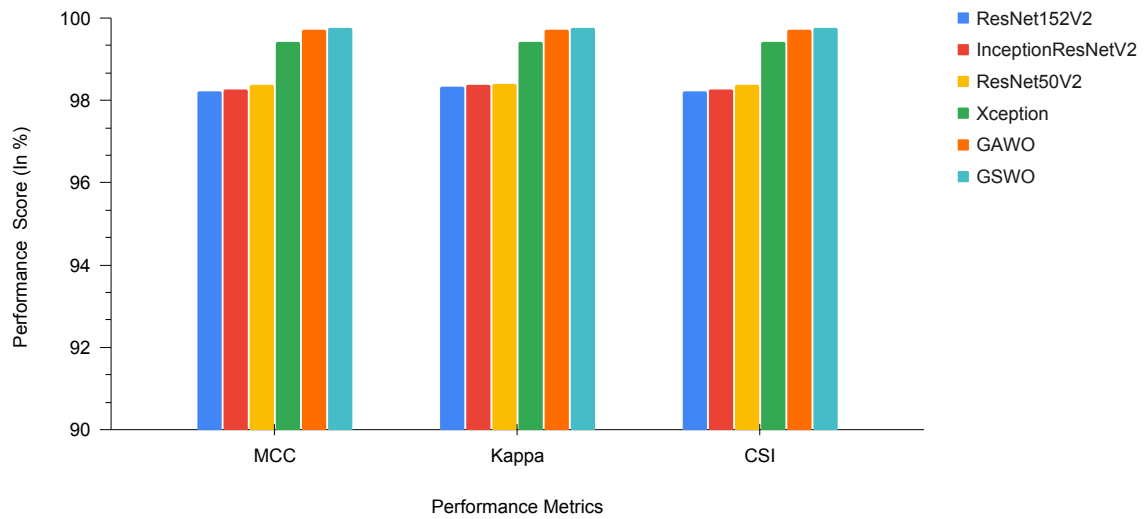
Likewise, in 7(b), the performance metrics are further elaborated. The MCC values for Xception, ResNet50V2, ResNet152V2, InceptionResNetV2, GAWO, and GSWO are recorded as 99.42%, 98.37%, 98.22%, 98.26%, 99.71%, and 99.76%, respectively. Additionally, the Kappa scores for these models are 99.43%, 98.41%, 98.34%, 98.37%, 99.71%, and 99.77%, and the CSI values are 99.42%, 98.37%, 98.22%, 98.26%, 99.71%, and 99.76%. Of all the models tested, GSWO demonstrates superior performance, achieving the highest MCC rate of 99.76%, Kappa score of 99.77%, and CSI rate of 99.76%.

Figure 8 presents the accuracy and loss trajectories for all the refined TL models. Throughout the training epochs, there is a noticeable increase in accuracy and a loss reduction, indicating effective learning. These learning curves reflect a solid training process, suggesting that the models successfully capture the input data’s nuances at each epoch. The strategy employed for data augmentation plays a crucial role in preventing overfitting. A detailed examination of the accuracy and loss graphs for each model is provided in the following section.

Xception: Observing Figure 8(a), it’s evident that the training and validation accuracy rates are consistently aligned, with training accuracy hovering around approximately 99.0% and validation accuracy around 98.4%. In Figure 8(b), the disparity between training and validation error rates is noticeable, with training loss at about 1.0% and validation loss around 1.6%. *ResNet50V2*: Figure 8(c) illustrates that the training and validation accuracy rates for ResNet50V2 are not as closely matched, with training accuracy near 99.0% and validation accuracy approximately 98.3%. Figure 8(d) shows a similar pattern in error rates, where training loss is around 1% and validation loss is near 1.7%. *ResNet152V2*: As depicted in Figure 8(e), there is a slight gap between the training and validation accuracy rates of ResNet152V2, with training accuracy close to 99.0% and validation accuracy about 98.2%. In Figure 8(f), this trend continues with the error rates, where training loss is approximately 1% and validation loss is around 1.8%. *InceptionResNetV2*: In Figure 8(g), the InceptionResNetV2 model shows a divergence in training and validation accuracy rates, with training accuracy around 99.0% and validation accuracy

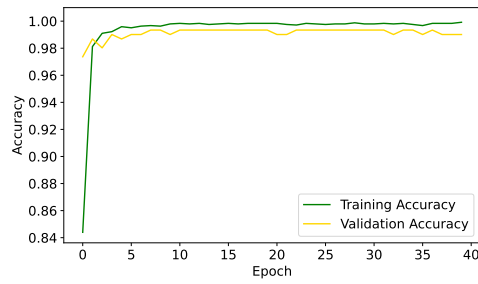


(a) Performance Analysis

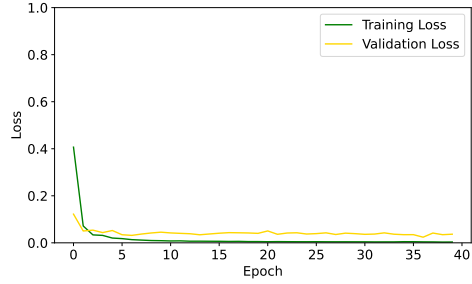


(b) Performance Analysis

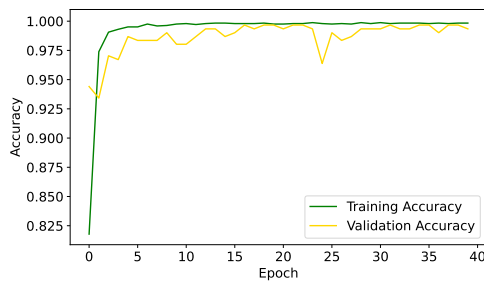
Figure 7: Performance Analysis of Proposed Models



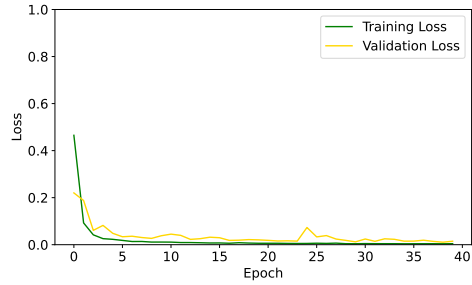
(a) Xception Accuracy



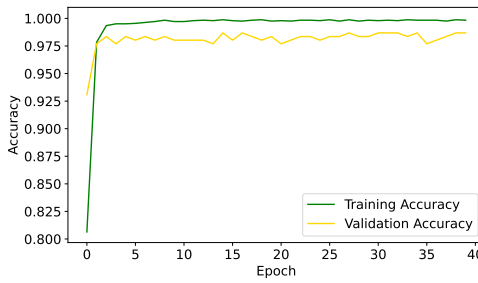
(b) Xception Loss



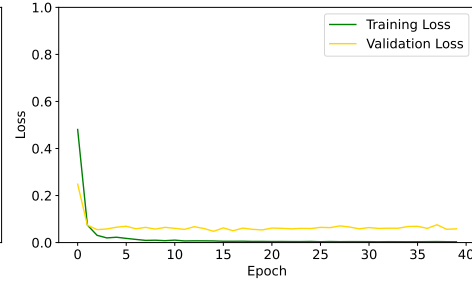
(c) ResNet50V2 Accuracy



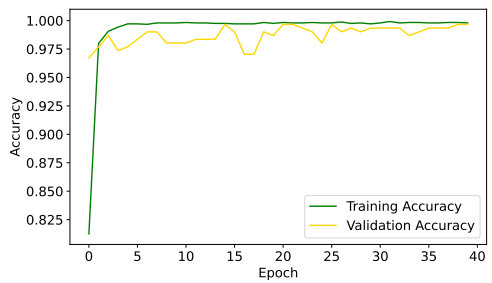
(d) ResNet50V2 Loss



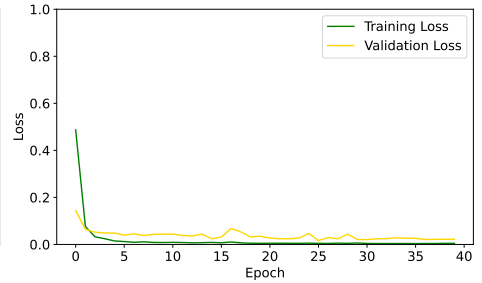
(e) ResNet152V2 Accuracy



(f) ResNet152V2 Loss



(g) InceptionResNetV2 Accuracy



(h) InceptionResNetV2 Loss

Figure 8: Accuracy and Loss Graphs for Proposed Models

near 98.2%. Figure 8(h) indicates a similar difference in error rates, with training loss at roughly 1% and validation loss about 1.8%.

Figure 9 displays the confusion matrices for all fine-tuned and optimized ensemble models. Below are the detailed breakdowns:

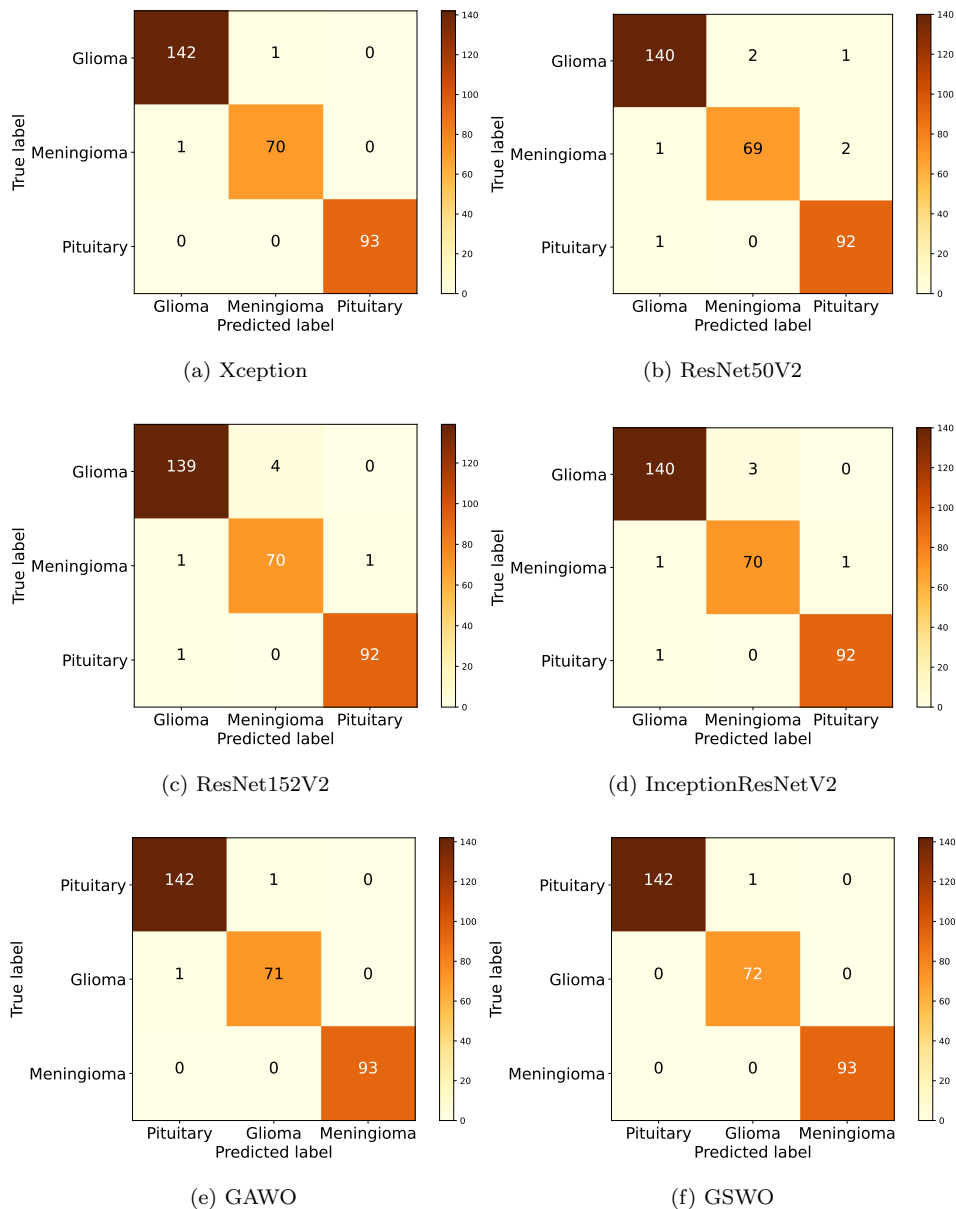


Figure 9: Comparative Confusion Matrices of Evaluated Models

For the Xception model (Figure 9(a)), the rates for glioma are TP: 46.25%, TN: 53.09%, FP: 0.33%, FN: 0.33%. For meningioma, TP: 22.80%, TN: 76.55%, FP: 0.33%, FN: 0.33%; and for pituitary, TP: 30.29%, TN: 69.71%, FP: 0.00%, FN: 0.00%. In the ResNet50V2 model (Figure 9(b)), glioma classification rates are TP: 45.45%, TN: 52.92%, FP: 0.65%, FN: 0.97%. For meningioma, TP: 22.40%, TN: 75.97%, FP: 0.65%, FN: 0.97%; and for pituitary, TP: 29.87%, TN: 68.83%, FP: 0.97%, FN: 0.32%. The ResNet152V2 model (Figure 9(c)) shows for glioma, TP: 45.13%,

TN: 52.92%, FP: 0.65%, FN: 1.30%. For meningioma, TP: 22.73%, TN: 75.32%, FP: 1.30%, FN: 0.65%; and for pituitary, TP: 29.87%, TN: 69.48%, FP: 0.32%, FN: 0.32%. In the InceptionResNetV2 model (Figure 9(d)), the glioma class rates are TP: 45.45%, TN: 52.92%, FP: 0.65%, FN: 0.97%. For meningioma, TP: 22.73%, TN: 75.65%, FP: 0.97%, FN: 0.65%; and for pituitary, TP: 29.87%, TN: 69.48%, FP: 0.32%, FN: 0.32%. The GAWO model (Figure 9(e)) presents for glioma, TP: 46.10%, TN: 53.25%, FP: 0.32%, FN: 0.32%. For meningioma, TP: 23.05%, TN: 76.30%, FP: 0.32%, FN: 0.32%; and for pituitary, TP: 30.19%, TN: 69.81%, FP: 0.00%, FN: 0.00%. Finally, in the GSWO model (Figure 9(f)), the rates for glioma are TP: 46.10%, TN: 53.57%, FP: 0.00%, FN: 0.32%. For meningioma, TP: 23.38%, TN: 76.30%, FP: 0.32%, FN: 0.00%; and for pituitary, TP: 30.19%, TN: 69.81%, FP: 0.00%, FN: 0.00%.

Upon evaluating the entire range of performance indicators, we have concluded that the GSWO model outperforms all other TL and ensemble optimization models. It has the lowest error rate and yields high rates of true positive and true negative results while generating fewer false positive and false negative results. The GSWO model offers superior performance scores to other models due to their meticulous exploration of weight combinations. By systematically searching through a grid of weights, GSWO optimally tunes the ensemble, adapting to the strengths of individual models. This method ensures that the ensemble leverages the diverse capabilities of each base model, leading to a more robust and accurate classification. The exhaustive weight search strategy of GSWO enhances the synergy among models, resulting in a finely tuned ensemble that excels in capturing intricate patterns in categorizing brain tumors, ultimately contributing to higher overall performance scores.

The classification report for categorizing brain tumors based on the proposed models is presented in Table 3. The table provides a detailed evaluation of the performance metrics, including precision, recall, and f1-score, for each class (glioma, meningioma, and pituitary) across different transfer learning algorithms (Xception, ResNet50V2, ResNet152V2, InceptionResNetV2) as well as optimization-based ensemble models (GAWO and GSWO).

Class Name	Xception			ResNet50V2			ResNet152V2			InceptionResNetV2			GAWO			GSWO		
	precision	recall	f1-score	precision	recall	f1-score	precision	recall	f1-score	precision	recall	f1-score	precision	recall	f1-score	precision	recall	f1-score
glioma	99.32	99.66	99.39	99.04	98.5	98.76	98.72	97.71	98.18	98.65	98.13	98.47	99.8	99.8	99.8	99.8	99.8	99.8
meningioma	99.32	98.44	98.78	97.63	96.55	97.06	95.43	97.95	96.59	96.05	98.04	96.86	99.4	99.4	99.4	99.4	99.6	99.6
pituitary	99.8	100	99.8	97.99	99.37	98.66	99.8	99.37	99.58	99.58	98.52	98.95	99.8	100	99.8	99.8	100	99.8
macro avg	99.41	99.37	99.39	98.15	98.27	98.1	97.98	98.21	98.05	98.23	98.23	98.09	99.6	99.6	99.6	99.8	99.8	99.8
weighted avg	99.4	99.4	99.4	98.44	98.42	98.42	98.39	98.29	98.3	98.44	98.35	98.17	99.8	99.8	99.8	99.8	99.8	99.8

Table 3: Classification Report for Proposed Models

For glioma classification, the Xception model achieved high precision (99.32%), recall (99.66%), and f1-score (99.39%), demonstrating its effectiveness. ResNet50V2 and ResNet152V2 also performed well, with f1-scores of 98.76% and 98.18%, respectively. The ensemble models GAWO and GSWO achieved outstanding results with precision, recall, and f1-score all at 99.8%. In meningioma classification, Xception and GAWO showed excellent precision, recall, and f1-score values, all above 99%. ResNet50V2 and ResNet152V2 exhibited slightly lower performance, with f1-scores of 97.06% and 96.59%, respectively. The GSWO ensemble model outperformed others with precision, recall, and f1-score, reaching 99.6%. For pituitary tumor classification, all models demonstrated exceptional performance with precision, recall, and f1-score values consistently above 97%. Xception and GAWO achieved perfect precision, recall, and f1-score at 100%, indicating their reliability in pituitary tumor classification.

The macro and weighted averages across all classes further emphasize the overall effectiveness of the proposed models. The weighted average f1-score for all models and ensembles is consistently high at 99.8%, highlighting the classification approach’s robustness for brain tumour types. These results underscore the potential of the proposed models for accurate and reliable categorizing brain tumours.

The consequence of the analysis demonstrates that the GSWO model outperforms others, achieving the highest accuracy at 99.76%. It is closely followed by the GAWO model with a 99.71% accuracy rate and the Xception model at 99.42%. The ResNet50V2, ResNet152V2, and InceptionResNetV2 models show accuracies of 98.37%, 98.22%, and 98.26% respectively. Additionally, these models excel in precision, recall, F1-score, MCC, Kappa, and CSI metrics. This indicates that the GSWO model stands as the most proficient ensemble DL model for classifying brain tumours.

4.4. Evaluation of Computational Complexity

In assessing the complexity of our experiments, we focused on the time taken for predictions, measured in seconds. These evaluations were conducted using an Intel Xeon CPU equipped with 3 Cores, 30GB of RAM, and a 30GB GPU. The scope of the study involved classifying brain tumors with a dataset containing 307 test images. The observed prediction times were as follows: Xception required 18 seconds, ResNet50V2 took 16 seconds, ResNet152V2 needed 20 seconds, InceptionResNetV2 was at 21 seconds, GAWO completed in 17 seconds, and notably, our GSWO model achieved the best performance with a time of 15 seconds. For a comprehensive breakdown of these times, Table 4 offers an in-depth view showcasing the results in tabular representations.

SI.No.	Proposed Model	Prediction Speed (In sec)
1	Xception	18
2	ResNet50V2	16
3	ResNet152V2	20
4	InceptionResNetV2	21
5	GAWO	17
6	GSWO	15

Table 4: Analysis of prediction speed of proposed models

4.5. Discussion

In our experiment, we executed preprocessing, reconfigured the architecture, and fine-tuned the model by incorporating additional layers, resulting in an optimized brain tumor detection model. Additionally, we have introduced optimization-based ensemble DL models to enhance the efficiency of categorizing brain tumors. Our optimized model for categorizing brain tumors has been rigorously assessed against existing methodologies, demonstrating a notably superior level of accuracy. The comparison study presented in Table 5 highlights the performance metrics of various categorizing brain tumor approaches. Notably, our proposal achieves the highest accuracy, reaching an impressive 99.76 percent, using the same brain tumor dataset Cheng (2017) and an equivalent number of images (3064). The utilization of identical datasets and image counts ensures a fair comparison for predicting efficiency. This study

SI. NO.	Authors	Techniques	Dataset Name	No. of Images	Accuracy (In %)
1	Talukder et al. (2023)	ResNet50V2	Brain tumor Cheng (2017)	3064	99.68
2	Saeedi et al. (2023)	2D CNN	Brain tumor Cheng (2017)	3064	96.47
3	Ayadi et al. (2021)	CNN	Brain tumor Cheng (2017)	3064	94.74
4	Sadad et al. (2021)	NASNet	Brain tumor Cheng (2017)	3064	99.60
5	Asif et al. (2023)	Xception	Brain tumor Cheng (2017)	3064	99.67
6	Nassar et al. (2023)	Majority Voting-Ensemble	Brain tumor Cheng (2017)	3064	99.31
2	Tummala et al. (2022)	Ensemble ViT	Brain tumor Cheng (2017)	3064	98.70
7	Abd El-Wahab et al. (2023)	BTC-fCNN	Brain tumor Cheng (2017)	3064	98.86
8	Maruf et al. (2022)	EfficientNetB3	Brain tumor Cheng (2017)	3064	98.98
9	Ait Amou et al. (2022)	Optimized CNN	Brain tumor Cheng (2017)	3064	98.70
10	Our Proposal	GSWO-Ensemble Model	Brain tumor Cheng (2017)	3064	99.76

Table 5: The comparison analysis of categorizing brain tumors on Figshare MRI Image Dataset

underscores the efficacy of GSWO, showcasing its ability to achieve unparalleled accuracy rates in categorizing brain tumors.

4.6. Potential Impact in Healthcare and Society

The core objective of our study is the development of an advanced deep-learning model dedicated to accurately classifying brain tumors, utilizing the strengths of deep learning to discern various tumor types with high precision. The potential impacts of this research are extensive, particularly in neuro-oncology, encompassing several clinically significant applications. Firstly, it offers an improved diagnostic tool for radiologists and medical professionals, aiding in the accurate diagnosis of brain tumors through techniques such as MRI scans. By providing reliable tumor categorization, the model reduces diagnostic errors and promotes early detection, thereby improving patient treatment outcomes. Additionally, the precise identification of tumor types facilitates the formulation of tailored treatment plans, ensuring patients receive targeted therapies that are more effective, thereby enhancing overall healthcare quality. Moreover, the model serves as a critical support tool in clinical decision-making processes, furnishing healthcare professionals with accurate information for better patient management and delivering more personalized patient care. Furthermore, by accurately classifying brain tumors and identifying specific genetic markers or molecular profiles, the model significantly contributes to brain tumor research, aiding in understanding tumor biology, identifying therapeutic targets, and advancing the development of optimized treatments and medications. In summary, our research offers substantial benefits in enhancing brain tumor diagnosis and treatment, supporting clinical decision-making, aiding surgical procedures, and advancing medical research, with the potential to positively influence both patient care and societal health outcomes.

5. Conclusion

This research presents a groundbreaking DL strategy specifically tailored for the accurate categorization of brain tumors. It integrates a series of steps including preprocessing, revamping TL frameworks, meticulous fine-tuning, and the application of optimized ensemble DL models. Our approach utilizes four TL algorithms - Xception,

ResNet50V2, ResNet152V2, and InceptionResNetV2 - along with two advanced optimization models, GAWO and GSWO. The study was conducted using the comprehensive Figshare MRI brain tumor image dataset. The assessment of our model was thorough, covering a wide array of performance indicators such as accuracy, recall, precision, f1 score, confusion matrix, MCC, Kappa, and CSI. Notably, the models achieved high classification accuracy, with Xception at 99.42%, ResNet50V2 at 99.37%, ResNet152V2 at 98.22%, InceptionResNetV2 at 98.26%, GAWO at 99.71%, and GSWO leading the pack at 99.76%. GSWO, in particular, stood out for its exceptional precision and recall, demonstrating its effectiveness and reliability in brain tumor detection. Nevertheless, the study acknowledges certain constraints, particularly related to image resolution, and highlights the ongoing need for enhancements in image processing and the DL model itself.

Our future endeavors include advancing our ensemble DL model by incorporating more sophisticated feature fusion techniques leveraging recently available brain tumor datasets. Additionally, we aim to enhance the interpretability of our model by integrating explainable AI techniques. This strategic evolution seeks to provide deeper insights into decision-making, fostering increased confidence and trust among clinicians and patients in the diagnostic realm.

Declarations

Conflict of interest

The authors have no conflicts of interest to declare that they are relevant to the content of this article.

Availability of data and materials

The selected datasets are sourced from free and open-access sources such as Figshare MRI Brain tumor Dataset: https://figshare.com/articles/dataset/brain_tumor_dataset/1512427.

Funding Statement

There is no funding available for this research.

Acknowledgments

This work is supported by the Information and Communication Technology (ICT) Fellowship Program of the ICT Division, Bangladesh, Fiscal Year 2022-2023 (GO No. 56.00.0000.052.33.004.22-06).

References

- Abd El-Wahab, B. S., Nasr, M. E., Khamis, S., and Ashour, A. S. (2023). Btc-fcnn: Fast convolution neural network for multi-class brain tumor classification. *Health Information Science and Systems*, 11(1):3.
- Ait Amou, M., Xia, K., Kamhi, S., and Mouhafid, M. (2022). A novel mri diagnosis method for brain tumor classification based on cnn and bayesian optimization. In *Healthcare*, volume 10, page 494. MDPI.
- Al-Azzwi, Z. H. N. and Nazarov, A. (2023). Brain tumor classification based on improved stacked ensemble deep learning methods. *Asian Pacific journal of cancer prevention: APJCP*, 24(6):2141.

- Al-Zoghby, A. M., Al-Awadly, E. M. K., Moawad, A., Yehia, N., and Ebada, A. I. (2023). Dual deep cnn for tumor brain classification. *Diagnostics*, 13(12):2050.
- Ale, Y. and Nainwal, N. (2023). Progress and challenges in the diagnosis and treatment of brain cancer using nanotechnology. *Molecular Pharmaceutics*, 20(10):4893–4921.
- Alemu, B. S., Feisso, S., Mohammed, E. A., and Salau, A. O. (2023). Magnetic resonance imaging-based brain tumor image classification performance enhancement. *Scientific African*, 22:e01963.
- Andreas, A., Mavromoustakis, C. X., Song, H., and Batalla, J. M. (2023). Optimisation of cnn through transferable online knowledge for stress and sentiment classification. *IEEE Transactions on Consumer Electronics*.
- Asif, S., Yi, W., Ain, Q. U., Hou, J., Yi, T., and Si, J. (2022). Improving effectiveness of different deep transfer learning-based models for detecting brain tumors from mr images. *IEEE Access*, 10:34716–34730.
- Asif, S., Zhao, M., Tang, F., and Zhu, Y. (2023). An enhanced deep learning method for multi-class brain tumor classification using deep transfer learning. *Multimedia Tools and Applications*, pages 1–28.
- Ayadi, W., Elhamzi, W., Charfi, I., and Atri, M. (2021). Deep cnn for brain tumor classification. *Neural Processing Letters*, 53(1):671–700.
- Benitez, C. M., Chuong, M. D., Künzel, L. A., and Thorwarth, D. (2024). Mri-guided adaptive radiation therapy. In *Seminars in Radiation Oncology*, volume 34, pages 84–91. Elsevier.
- Bhosale, Y. H. and Patnaik, K. S. (2023). Puldi-covid: Chronic obstructive pulmonary (lung) diseases with covid-19 classification using ensemble deep convolutional neural network from chest x-ray images to minimize severity and mortality rates. *Biomedical Signal Processing and Control*, 81:104445.
- Bonate, P. L., Barrett, J. S., Ait-Oudhia, S., Brundage, R., Corrigan, B., Duffull, S., Gastonguay, M., Karlsson, M. O., Kijima, S., Krause, A., et al. (2023). Training the next generation of pharmacometric modelers: a multisector perspective. *Journal of pharmacokinetics and pharmacodynamics*, pages 1–27.
- Cerbone, M., Dattani, M., Maghnie, M., and Patti, G. (2023). Hypothalamo-pituitary disorders in childhood and adolescence. In *Paediatric Endocrinology: Management of Endocrine Disorders in Children and Adolescents*, pages 1–48. Springer.
- Chadha, R. and Verma, R. K. (2023). Application of artificial intelligence and deep learning in healthcare. In *Computational Health Informatics for Biomedical Applications*, pages 87–112. Apple Academic Press.
- Cheng, J. (2017). Brain magnetic resonance imaging tumor dataset. *Figshare MRI Dataset Version*, 5.
- Chollet, F. (2017). Xception: Deep learning with depthwise separable convolutions. In *Proceedings of the IEEE conference on computer vision and pattern recognition*, pages 1251–1258.
- Chopra, H., Shin, D. K., Munjal, K., Dhama, K., Emran, T. B., et al. (2023). Revolutionizing clinical trials: the role of ai in accelerating medical breakthroughs. *International Journal of Surgery*, 109(12):4211–4220.

- Cinar, N., Kaya, M., and Kaya, B. (2023). A novel convolutional neural network-based approach for brain tumor classification using magnetic resonance images. *International Journal of Imaging Systems and Technology*, 33(3):895–908.
- Dewi, C., Christanto, H., and Dai, G. (2023). Automated identification of insect pests: A deep transfer learning approach using resnet. *Acadlore Trans. Mach. Learn*, 2(4):194–203.
- Duan, J., Xie, S., Sun, H., An, J., Li, H., Li, L., Grimm, R., Voskrebenezv, A., and Vogel-Claussen, J. (2023). Diagnostic accuracy of perfusion-weighted phase-resolved functional lung magnetic resonance imaging in patients with chronic pulmonary embolism. *Frontiers in Medicine*, 10.
- Emam, M. M., Samee, N. A., Jamjoom, M. M., and Houssein, E. H. (2023). Optimized deep learning architecture for brain tumor classification using improved hunger games search algorithm. *Computers in Biology and Medicine*, 160:106966.
- Engelen, T., Solcà, M., and Tallon-Baudry, C. (2023). Interoceptive rhythms in the brain. *Nature Neuroscience*, 26(10):1670–1684.
- Fares, J., Petrosyan, E., Kanojia, D., Dmello, C., Cordero, A., Duffy, J. T., Yeeravalli, R., Sahani, M. H., Zhang, P., Rashidi, A., et al. (2023). Metixene is an incomplete autophagy inducer in preclinical models of metastatic cancer and brain metastases. *The Journal of Clinical Investigation*, 133(24).
- Hasan, I., Roy, S., Guo, B., and Chang, C. (2023). Parkinson’s disease: Current status, diagnosis, and treatment using nanomedicines. *Advanced Therapeutics*, 6(9):2300058.
- He, K., Zhang, X., Ren, S., and Sun, J. (2016a). Deep residual learning for image recognition. In *Proceedings of the IEEE conference on computer vision and pattern recognition*, pages 770–778.
- He, K., Zhang, X., Ren, S., and Sun, J. (2016b). Identity mappings in deep residual networks. In *European conference on computer vision*, pages 630–645. Springer.
- Joseph, F. J. J., Nonsiri, S., and Monsakul, A. (2021). Keras and tensorflow: A hands-on experience. *Advanced Deep Learning for Engineers and Scientists: A Practical Approach*, pages 85–111.
- Kimberly, W. T., Sorby-Adams, A. J., Webb, A. G., Wu, E. X., Beekman, R., Bowry, R., Schiff, S. J., de Havenon, A., Shen, F. X., Sze, G., et al. (2023). Brain imaging with portable low-field mri. *Nature Reviews Bioengineering*, 1(9):617–630.
- Kumar, S. and Kumar, D. (2023). Human brain tumor classification and segmentation using cnn. *Multimedia Tools and Applications*, 82(5):7599–7620.
- Kumar, S., Parthasarathi, P., Hogo, M. A., Masud, M., Al-Amri, J. F., and Abouhawwash, M. (2023). Breast cancer detection using breastnet-18 augmentation with fine tuned vgg-16. *Intelligent Automation and Soft Computing*, 36(2):2363–2378.

- Kumari, J., Kumar, E., and Kumar, D. (2023). A structured analysis to study the role of machine learning and deep learning in the healthcare sector with big data analytics. *Archives of Computational Methods in Engineering*, pages 1–29.
- Li, Z., Zou, J., and Chen, X. (2023). In response to precision medicine: Current subcellular targeting strategies for cancer therapy. *Advanced Materials*, 35(21):2209529.
- Luckett, P. H., Olufawo, M., Lamichhane, B., Park, K. Y., Dierker, D., Verastegui, G. T., Yang, P., Kim, A. H., Chheda, M. G., Snyder, A. Z., et al. (2023). Predicting survival in glioblastoma with multimodal neuroimaging and machine learning. *Journal of Neuro-oncology*, 164(2):309–320.
- Maruf, A., Taofeeq, I. A., Udunna, A., Michael, A. O., Adetunji, A., Adekunle, A., and Moses, A. (2022). Evaluating the performance of transfer-learning approaches for multiclass classification of glioma, meningioma and pituitary tumour. *African Journal of Medical Physics*, 4(1).
- Marx, W., Manger, S. H., Blencowe, M., Murray, G., Ho, F. Y.-Y., Lawn, S., Blumenthal, J. A., Schuch, F., Stubbs, B., Ruusunen, A., et al. (2023). Clinical guidelines for the use of lifestyle-based mental health care in major depressive disorder: World federation of societies for biological psychiatry (wfsbp) and australasian society of lifestyle medicine (aslm) taskforce. *The World Journal of Biological Psychiatry*, pages 1–54.
- Muezzinoglu, T., Baygin, N., Tuncer, I., Barua, P. D., Baygin, M., Dogan, S., Tuncer, T., Palmer, E. E., Cheong, K. H., and Acharya, U. R. (2023). Patchresnet: Multiple patch division-based deep feature fusion framework for brain tumor classification using mri images. *Journal of Digital Imaging*, pages 1–15.
- Mukhatov, A., Le, T.-A., Pham, T. T., and Do, T. D. (2023). A comprehensive review on magnetic imaging techniques for biomedical applications. *Nano Select*, 4(3):213–230.
- Nassar, S. E., Yasser, I., Amer, H. M., and Mohamed, M. A. (2023). A robust mri-based brain tumor classification via a hybrid deep learning technique. *The Journal of Supercomputing*, pages 1–25.
- Nizamani, A. H., Chen, Z., Nizamani, A. A., and Shaheed, K. (2023). Feature-enhanced fusion of u-net-based improved brain tumor images segmentation. *Journal of Cloud Computing*, 12(1):170.
- Prencipe, N., Marinelli, L., Varaldo, E., Cuboni, D., Berton, A. M., Bioletto, F., Bona, C., Gasco, V., and Grottoli, S. (2023). Isolated anterior pituitary dysfunction in adulthood. *Frontiers in Endocrinology*, 14:1100007.
- Qureshi, I., Yan, J., Abbas, Q., Shaheed, K., Riaz, A. B., Wahid, A., Khan, M. W. J., and Szczuko, P. (2023). Medical image segmentation using deep semantic-based methods: A review of techniques, applications and emerging trends. *Information Fusion*, 90:316–352.
- Rahimzadeh, M. and Attar, A. (2020). A modified deep convolutional neural network for detecting covid-19 and pneumonia from chest x-ray images based on the concatenation of xception and resnet50v2. *Informatics in medicine unlocked*, 19:100360.

- Rakshit, P., Chatterjee, S., Halder, C., Sen, S., Obaidullah, S. M., and Roy, K. (2023). Comparative study on the performance of the state-of-the-art cnn models for handwritten bangla character recognition. *Multimedia Tools and Applications*, 82(11):16929–16950.
- Rastogi, D., Johri, P., Tiwari, V., and Elngar, A. A. (2024). Multi-class classification of brain tumour magnetic resonance images using multi-branch network with inception block and five-fold cross validation deep learning framework. *Biomedical Signal Processing and Control*, 88:105602.
- Sadad, T., Rehman, A., Munir, A., Saba, T., Tariq, U., Ayesha, N., and Abbasi, R. (2021). Brain tumor detection and multi-classification using advanced deep learning techniques. *Microscopy Research and Technique*, 84(6):1296–1308.
- Saeedi, S., Rezayi, S., Keshavarz, H., and R. Niakan Kalhori, S. (2023). Mri-based brain tumor detection using convolutional deep learning methods and chosen machine learning techniques. *BMC Medical Informatics and Decision Making*, 23(1):16.
- Salari, N., Ghasemi, H., Fatahian, R., Mansouri, K., Dokaneheifard, S., Shiri, M. H., Hemmati, M., and Mohammadi, M. (2023). The global prevalence of primary central nervous system tumors: a systematic review and meta-analysis. *European journal of medical research*, 28(1):39.
- Sharma, A. K., Nandal, A., Dhaka, A., Zhou, L., Alhudhaif, A., Alenezi, F., and Polat, K. (2023). Brain tumor classification using the modified resnet50 model based on transfer learning. *Biomedical Signal Processing and Control*, 86:105299.
- Singh, R. and Agarwal, B. B. (2023). An automated brain tumor classification in mr images using an enhanced convolutional neural network. *International Journal of Information Technology*, 15(2):665–674.
- Szegedy, C., Ioffe, S., Vanhoucke, V., and Alemi, A. A. (2017). Inception-v4, inception-resnet and the impact of residual connections on learning. In *Thirty-first AAAI conference on artificial intelligence*.
- Talukder, M. A., Hossen, R., Uddin, M. A., Uddin, M. N., and Acharjee, U. K. (2024a). Securing transactions: A hybrid dependable ensemble machine learning model using iht-lr and grid search. *Cybersecurity arXiv:2402.14389*.
- Talukder, M. A., Islam, M. M., Uddin, M. A., Akhter, A., Hasan, K. F., and Moni, M. A. (2022). Machine learning-based lung and colon cancer detection using deep feature extraction and ensemble learning. *Expert Systems with Applications*, 205:117695.
- Talukder, M. A., Islam, M. M., Uddin, M. A., Akhter, A., Pramanik, M. A. J., Aryal, S., Almoyad, M. A. A., Hasan, K. F., and Moni, M. A. (2023). An efficient deep learning model to categorize brain tumor using reconstruction and fine-tuning. *Expert Systems with Applications*, page 120534.
- Talukder, M. A., Islam, M. M., Uddin, M. A., Hasan, K. F., Sharmin, S., Alyami, S. A., and Moni, M. A. (2024b). Machine learning-based network intrusion detection for big and imbalanced data using oversampling, stacking feature embedding and feature extraction. *Journal of Big Data*, 11(1):1–44.

- Talukder, M. A., Layek, M. A., Kazi, M., Uddin, M. A., and Aryal, S. (2024c). Empowering covid-19 detection: Optimizing performance through fine-tuned efficientnet deep learning architecture. *Computers in Biology and Medicine*, 168:107789.
- Talukder, M. A., Sharmin, S., Uddin, M. A., Islam, M. M., and Aryal, S. (2024d). Mlstl-wsn: machine learning-based intrusion detection using smotetomek in wsns. *International Journal of Information Security*, pages 1–20.
- Tian, Y., Zeng, Z., Wen, M., Liu, Y., Kuo, T.-y., and Cheung, S.-C. (2020). Evaldnn: A toolbox for evaluating deep neural network models. In *Proceedings of the ACM/IEEE 42nd International Conference on Software Engineering: Companion Proceedings*, pages 45–48.
- Tseng, C.-J. and Tang, C. (2023). An optimized xgboost technique for accurate brain tumor detection using feature selection and image segmentation. *Healthcare Analytics*, 4:100217.
- Tummala, S., Kadry, S., Bukhari, S. A. C., and Rauf, H. T. (2022). Classification of brain tumor from magnetic resonance imaging using vision transformers ensembling. *Current Oncology*, 29:7498 – 7511.
- You, K., Kou, Z., Long, M., and Wang, J. (2020). Co-tuning for transfer learning. *Advances in Neural Information Processing Systems*, 33:17236–17246.
- Zheng, Y., Huang, Y., Luo, J., Peng, X., Gui, X., Liu, G., and Zhang, Y. (2023). Supercritical fluid technology: A game-changer for biomacromolecular nanomedicine preparation and biomedical application. *Chinese Chemical Letters*, page 109169.
- Zulfiqar, F., Bajwa, U. I., and Mehmood, Y. (2023). Multi-class classification of brain tumor types from mr images using efficientnets. *Biomedical Signal Processing and Control*, 84:104777.